

Supporting Information

Optimized nanospace of coordination isomers with selenium site for acetylene separation

Huijie Wang,^a Nibedita Behera,^a Suna Wang,^b Qiubing Dong,^a Zhaoxu Wang,^c Baishu Zheng,^c Daqi Wang,^b and Jingui Duan^{a,*}

^aState Key Laboratory of Materials-Oriented Chemical Engineering, College of Chemical Engineering, Nanjing Tech University, Nanjing 210009, China. Email: duanjingui@njtech.edu.cn.

^bShandong Provincial Key Laboratory of Chemical Energy Storage and Novel Cell Technology, School of Chemistry and Chemical Engineering, Liaocheng University, Liaocheng 252059, China.

^c Key Laboratory of Theoretical Organic Chemistry and Function Molecule of Ministry of Education, Hunan Provincial Key Laboratory of Controllable Preparation and Functional Application of Fine Polymers, Hunan Provincial Key Laboratory of Advanced Materials for New Energy Storage and Conversion, School of Chemistry and Chemical Engineering, Hunan University of Science and Technology, Xiangtan 411201, China.

General procedures and materials

All the solvents and materials were purchased from chemical vendors and without further depuration before used. The instrument used for the ^1H -NMR test was a Bruker Advance III 600 MHz nuclear magnetic resonance spectrometer. Powder X-Ray Diffraction (PXRD) pattern was tested with Bruker AXS D8 Advance (test conditions: 40 kV, 40 mA, $\text{CuK}\alpha$, $\lambda = 1.5418 \text{ \AA}$, scanning range $5\text{--}50^\circ$). Infrared (FT-IR) spectra were tested on the VECTOR 22 spectrometer using KBr tableting method in the range of $4000\text{--}400 \text{ cm}^{-1}$. Thermogravimetric analysis (TGA) measurements were performed on a STA 209 F1 instrument under astatic N_2 atmosphere with a heating rate of $10 \text{ }^\circ\text{C}/\text{min}$ at the range of $30\text{--}650 \text{ }^\circ\text{C}$.

Crystallography

Single-crystal X-ray diffraction data was collected by a Bruker Smart Apex CCD diffractometer at 298 K using graphite monochromator $\text{Mo K}\alpha$ radiation ($\lambda = 0.71073 \text{ \AA}$). Data reduction was made with the Bruker SAINT program. The structure was solved by direct methods and refined with full-matrix least-squares technique using the SHELXTL package. Non-hydrogen atoms were refined with anisotropic displacement parameters during the final cycles. Organic hydrogen atoms were placed in calculated positions with isotropic displacement parameters set to $1.2 \times U_{\text{eq}}$ of the attached atom. We have employed PLATON/SQUEEZE to calculate the diffraction contribution of the solvent molecules and, thereby, to produce a set of solvent-free diffraction intensities; structures were then refined again using the data generated. Crystal data are summarized in ESI, Table S1.

Sample activation

Prior to adsorption measurement, the samples were prepared by immersing the as-synthesized samples in ethanol for three days to remove non-volatile solvents, and the extract was decanted every 8 h and replaced with fresh ethanol. The completely activated sample was obtained by heating the solvent-exchanged sample at 120°C under a dynamic high vacuum for 20 h.

Single gas adsorption

In the gas adsorption measurement, ultra-high-purity grade of N_2 , C_2H_2 , and CO_2 gases were used throughout the adsorption experiments. Gas adsorption isotherms were obtained using a Belsorp-mini volumetric adsorption instrument from BEL Japan Inc, using the volumetric technique.

Binary mixture adsorption.

IAST was used to predict binary mixture adsorption from the experimental pure-gas isotherms. In order to perform the integrations required by IAST, the single-component isotherms were fitted

by the dual-site Langmuir-Freundlich equation:

$$q = q_{m1} \cdot \frac{b_1 \cdot P^{1/n_1}}{1 + b_1 \cdot P^{1/n_1}} + q_{m2} \cdot \frac{b_2 \cdot P^{1/n_2}}{1 + b_2 \cdot P^{1/n_2}} \quad (1)$$

Here, P is the pressure of the bulk gas at equilibrium with the adsorbed phase (kPa), q is the adsorbed amount per mass of adsorbent (mol/kg), q_{m1} and q_{m2} are the saturation capacities of sites 1 and 2 (mol/kg), b_1 and b_2 are the affinity coefficients of sites 1 and 2 (1/kPa), and n_1 and n_2 represent the deviations from an ideal homogeneous surface. Figure 4c shows that the dual-site Langmuir-Freundlich equation fits the single-component isotherms extremely well. The R_2 values for all the fitted isotherms were over 0.99997. Hence, the fitted isotherm parameters were applied to perform the necessary integrations in IAST.

Estimation of the adsorption heats

A virial-type expression comprising the temperature-independent parameters a_i and b_i was employed to calculate the enthalpies of adsorption for C_2H_2 , and CO_2 (at 273, 283 and 298 K) on crystals. In each case, the data were fitted using the equation:

$$\ln P = \ln N + 1/T \sum_{i=0}^m a_i N^i + \sum_{i=0}^n b_i N^i \quad (2)$$

Here, P is the pressure expressed in Torr, N is the amount adsorbed in mmol/g, T is the temperature in K, a_i and b_i are virial coefficients, and m , n represents the number of coefficients required to adequately describe the isotherms (m and n were gradually increased until the contribution of extra added a and b coefficients was deemed to be statistically insignificant towards the overall fit, and the average value of the squared deviations from the experimental values was minimized):

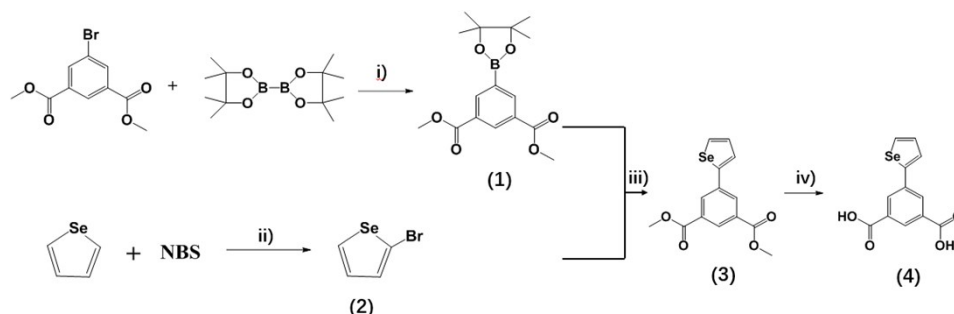
$$Q_{st} = -R \sum_{i=0}^m a_i N^i \quad (3)$$

Here, Q_{st} is the coverage-dependent isosteric heat of adsorption and R is the universal gas constant.

Stability test

Crystals of **NTU-57** and **NTU-58** were soaked in chemical solutions at pH =2 and 12 for 3 days and in water for one month. After this, the samples were examined by PXRD.

Ligand synthesis



Scheme S1. Synthetic routes for ligand H₂sip synthesis.

(i)

A mixture of dimethyl 5-bromoisophthalate (7.8 g, 28.6 mmol) and Borylborate (8.0 g, 31.4 mmol), KOAc (8.4 g, 85.7 mmol), PdCl₂(dppf) CH₂Cl₂ (0.6 g, 0.74 mmol) were taken in an empty round bottom flask and degassed the solid mixture for 15 min. under nitrogen atmosphere. After that, dry DMSO (60 mL) was added to the mixture and stirred at 80°C for 24 h under nitrogen atmosphere. The reaction mixture was poured into ice water (1000 mL) and filtered. The filtrate part was extracted with CH₂Cl₂ and collected to dry to get solid. Then, the solid residue was dissolved in CH₂Cl₂, extracted three times with water, and the collected organic phase was evaporated to dryness. Both the solids obtained from extraction was combined and purified by column chromatography to obtain **1** (6.07 g, 90.2%).

(ii)

A solution of selenophenol (2.62 g, 20 mmol) in CH₂Cl₂ (70 mL) was placed in ice water bath at 0 °C. Then, 30 drops of HBr was added slowly and also NBS (3.56 g, 20 mmol) into the solution. After complete addition, the reaction mixture was stirred for overnight at room temperature. The saturated solution of Na₂S₂O₃ (30 mL) was added to the reaction mixture, and stirred well. The resultant solution then extracted with CH₂Cl₂ and the collected organic phase was steamed (38°C) to obtain the yellow oil liquid **2** (3.18 g, 75.7%).

(iii)

A mixture of dimethyl 5-bromoisophthalate (3.2 g, 10 mmol) and 2-bromo selenophenol (2.1 g, 10 mmol), K₂CO₃ (2.12 g, 20 mmol), Pd(PPh₃)₄ (0.720 g, 0.6 mmol) were taken in an empty RB and dissolved in the mixture of solvents; toluene/methanol/water (100/40/5 mL) and degassed in presence of N₂ gas. The mixture was stirred at 85°C for 48 h under nitrogen atmosphere. After completion of reaction, the organic solvents were dried under vacuum and the residue was extracted with CH₂Cl₂ (3×100 mL). The organic phase was again washed with water (3 × 50 mL), dried with anhydrous MgSO₄, filtered and concentrated to dryness. The residue was purified by column chromatography to afford **3** (2.36 g, 72.3%). ¹H NMR (400 MHz, CDCl₃) δ 8.57 (t, *J* = 1.5 Hz,

1H), 8.39 (d, $J = 1.5$ Hz, 2H), 8.03 (dd, $J = 5.6, 1.0$ Hz, 1H), 7.62 (dd, $J = 3.8, 1.0$ Hz, 1H), 7.36 (dd, $J = 5.6, 3.8$ Hz, 1H), 3.98 (s, 6H).

(vi)

A solution of **3** (2 g, 6.13 mmol) in THF/MeOH (60/60 mL) was prepared and NaOH (4.9 g, 122.5 mmol) in water (120 mL) was added into it. The resulting mixture was refluxed for 16 h. The reaction mixture was evaporated and the residue was dissolved in water and filtered. A solution of HCl (3M) was added to the filtrate until a large amount of precipitates was appeared. The precipitates were collected by filtration, washed thoroughly with water and dried in vacuum to afford **H₂sip** (1.77 g, 97.4%) as an off-yellow powder. ¹H NMR (400 MHz, DMSO) δ 8.36 (d, $J = 1.4$ Hz, 1H), 8.29 (d, $J = 1.4$ Hz, 2H), 8.27 (d, $J = 5.5$ Hz, 1H), 7.86 – 7.82 (m, 1H), 7.40 (dd, $J = 5.5, 3.9$ Hz, 1H), 13.48 (bs, 2H).

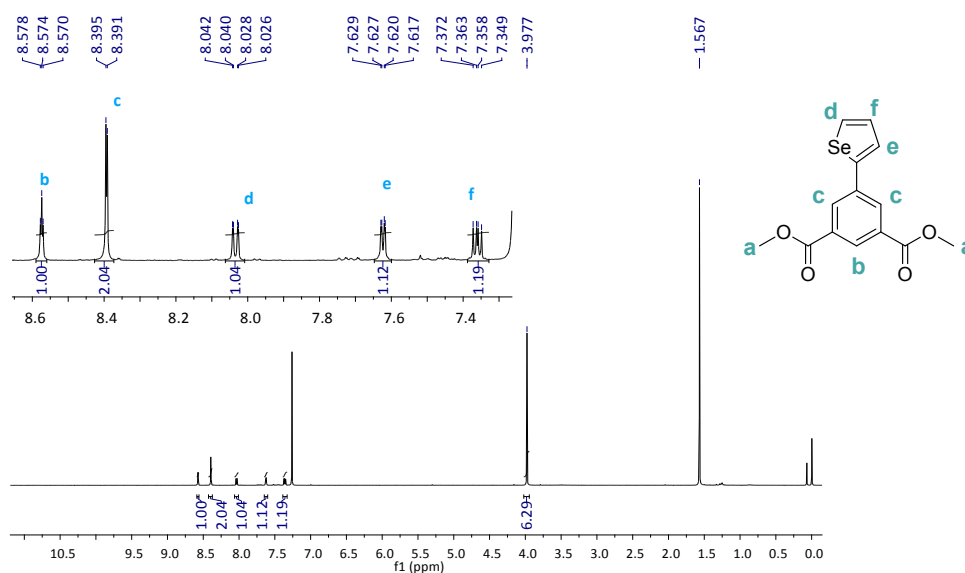


Figure S1 ¹H NMR spectrum of **3**.

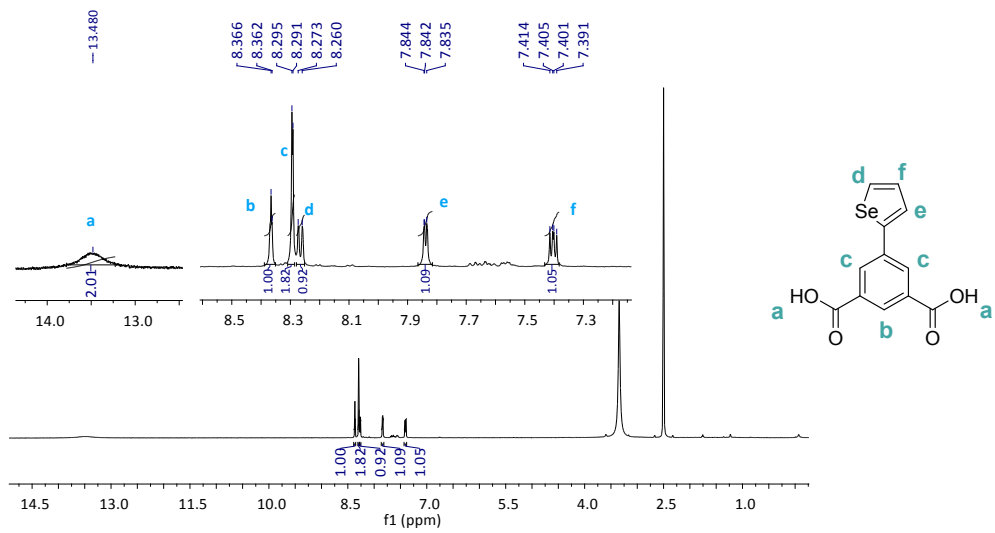


Figure S2 ^1H NMR spectrum of **4**.

Table S1. Crystal data and structure refinement parameters for **NTU-56** to **NTU-58**.

	NTU-56	NTU-57	NTU-58
Empirical formula	C ₁₂ H ₈ CuO ₅ Se	C ₁₂ H ₈ CuO ₅ Se	C ₁₂ H ₈ CuO ₅ Se
Formula weight	374.69	374.69	374.69
Space group	I212121	R -3	P-3m1
a / Å	10.889(3)	18.3147(12)	18.8359(13)
b / Å	11.187(3)	18.3147(12)	18.8359(13)
c / Å	30.229(7)	22.670(3)	7.1622(10)
β / °	90	90	90
V/Å³	3466(6)	6949(2)	2113.7(6)
Z	8	18	6
D_{calc}/gcm⁻³	1.352	1.612	1.696
μ/mm⁻¹	3.171	3.78	3.980
θ range^o	1.9, 25.1	1.5, 25.0	1.3, 25.1
Index ranges	-12 ≤ h ≤ 12 -13 ≤ k ≤ 13 -36 ≤ l ≤ 32	-22 ≤ h ≤ 20 -22 ≤ k ≤ 22 -27 ≤ l ≤ 27	-22 ≤ h ≤ 22 -21 ≤ k ≤ 22 -8 ≤ l ≤ 8
R₁	0.0699	0.1479	0.0798
wR_{2a}[I > 2σ(I)]	0.1990	0.5372	0.2493
GOF	1.04	1.07	1.08

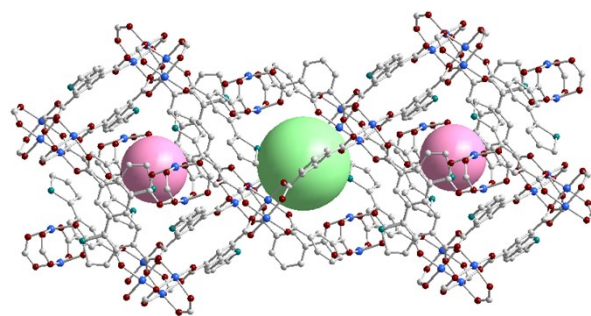


Figure S3 Two cages highlighted by pink and green ball of **NTU-57**. The diameters of them are 4.0 and 5.0 Å, respectively.

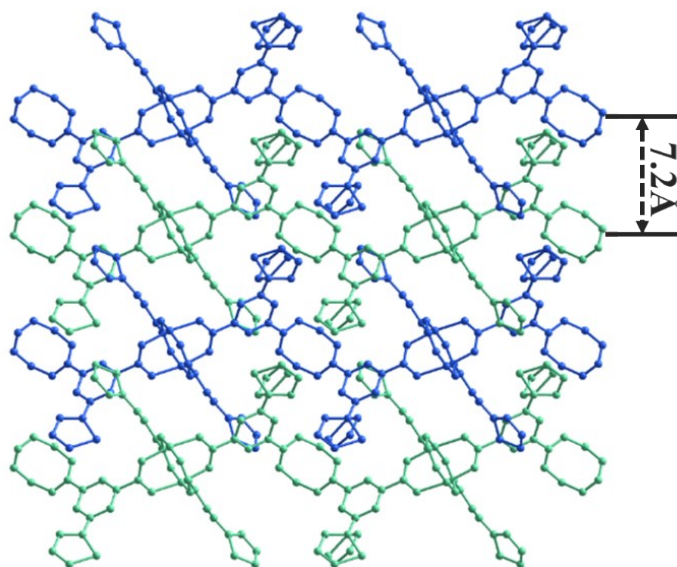


Figure S4 Side view of stacked **NTU-58**.

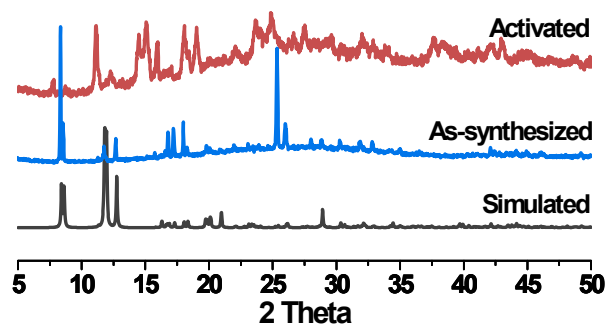


Figure S5 XRD patterns of NTU-56.

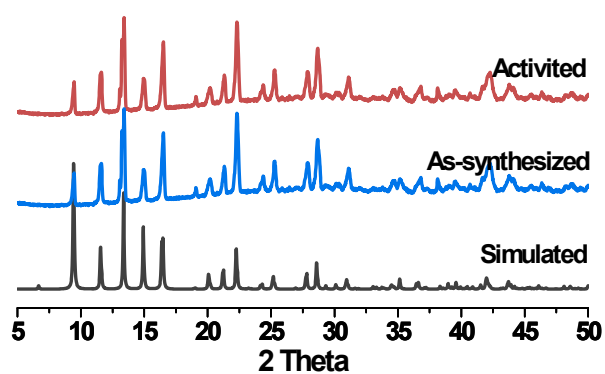


Figure S6 XRD patterns of NTU-57.

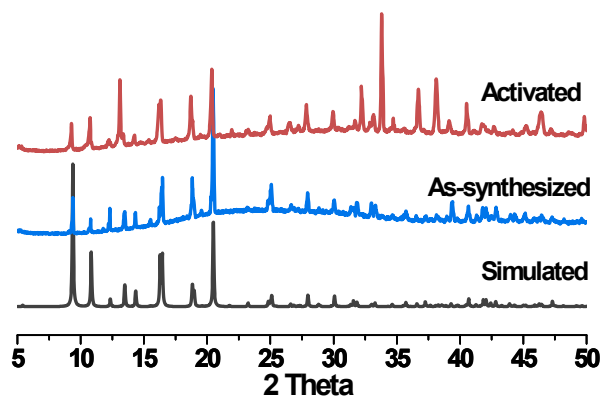


Figure S7 XRD patterns of NTU-58.

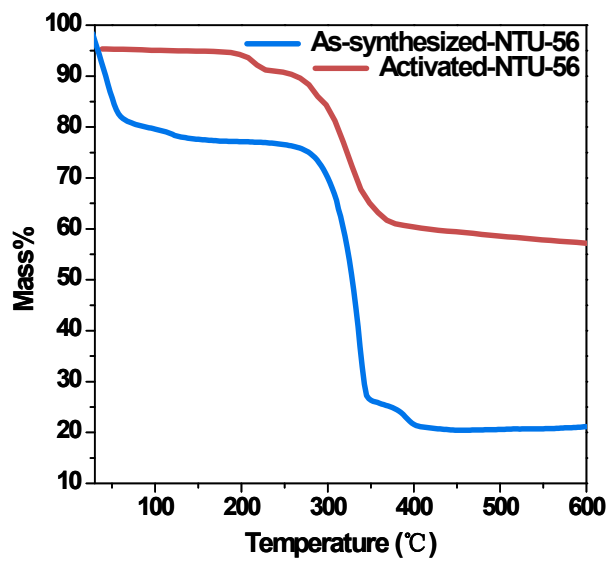


Figure S8 TG patterns of NTU-56.

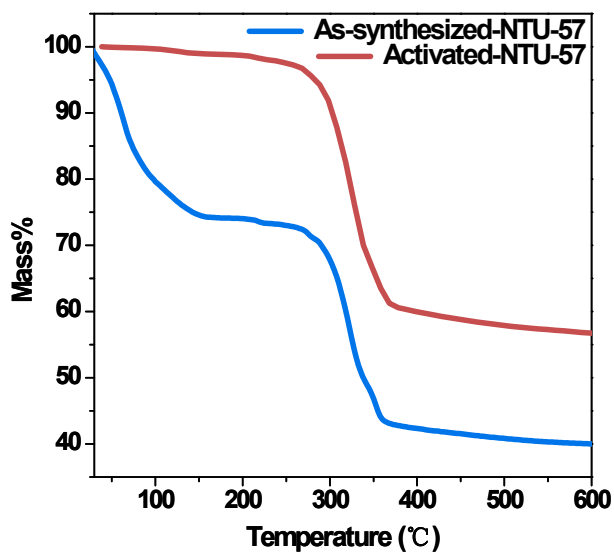


Figure S9 TG patterns of NTU-57.

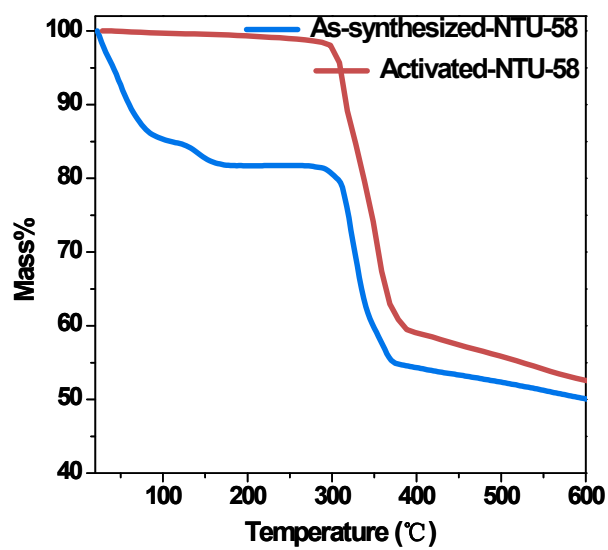


Figure S10 TG patterns of NTU-58.

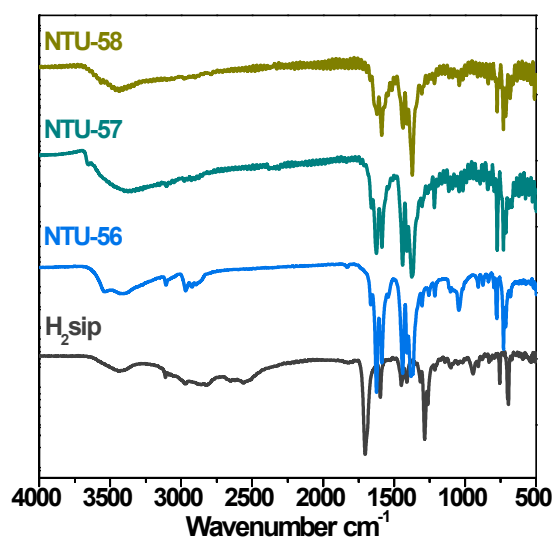


Figure S11 FT-IR spectra for the three PCPs and ligand.

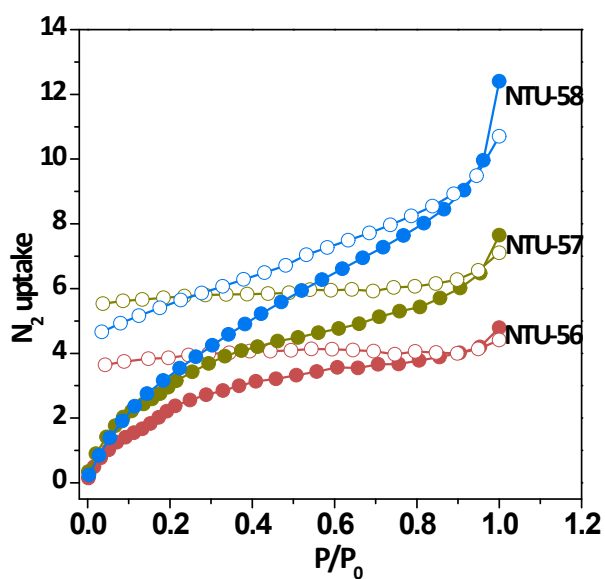


Figure S12 N_2 adsorption of NTU-56 to NTU-58 at 77K.

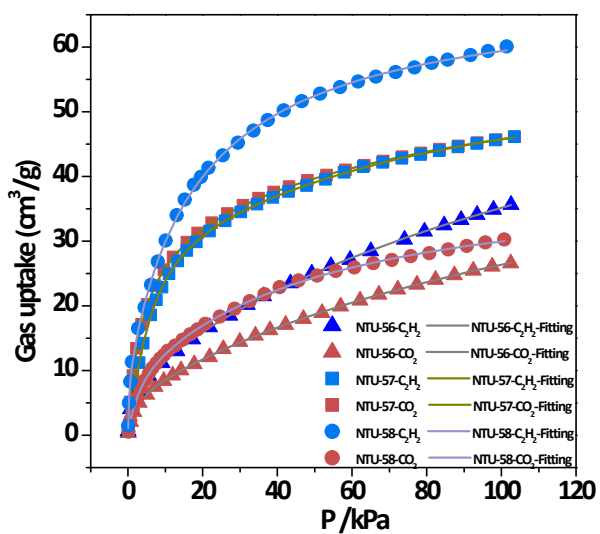


Figure S13 Adsorption isotherms of CO_2 and C_2H_2 for NTU-56 to NTU-58 at 273 K, 1 bar. Points and lines show the experimental data and corresponding dual-site Langmuir–Freundlich fitness, respectively.

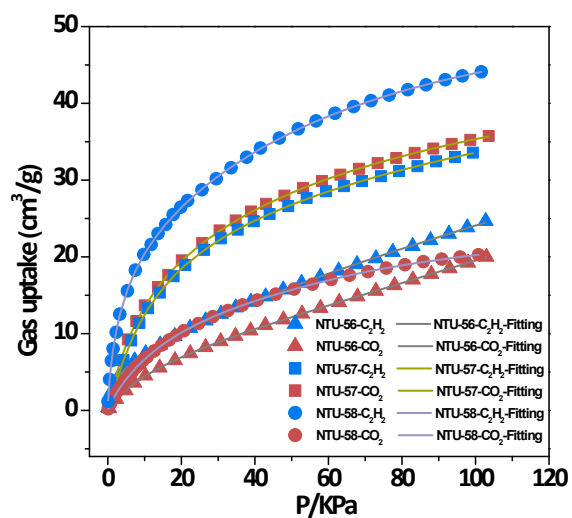


Figure S14 Adsorption isotherms of CO_2 and C_2H_2 for **NTU-56** to **NTU-58** at 298 K, 1 bar. Points and lines show the experimental data and corresponding dual-site Langmuir–Freundlich fitness, respectively.

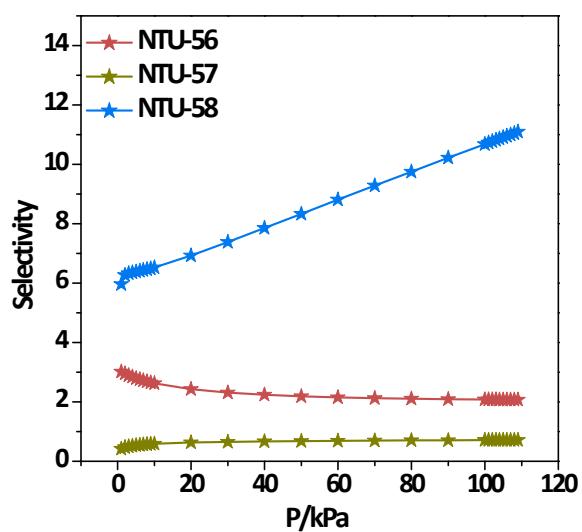


Figure S15 IAST selectivity of **NTU-56** to **NTU-58** from $\text{CO}_2/\text{C}_2\text{H}_2$ (50/50) gas mixtures at 298 K.

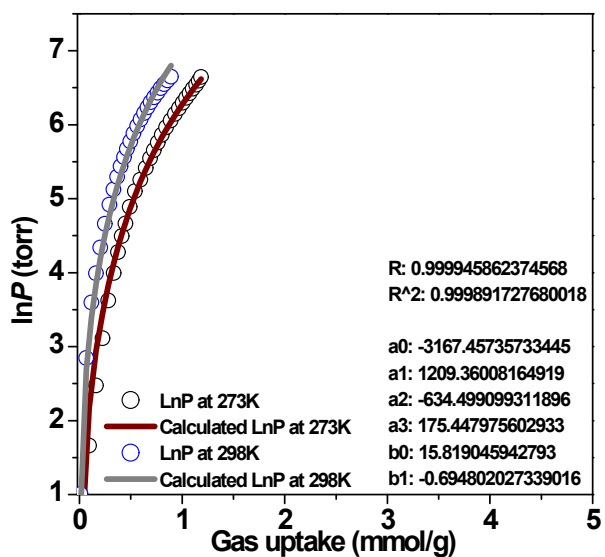


Figure S16 Curves fitting of CO₂ gas adsorption isotherms for NTU-56 at 273 K and 298 K.

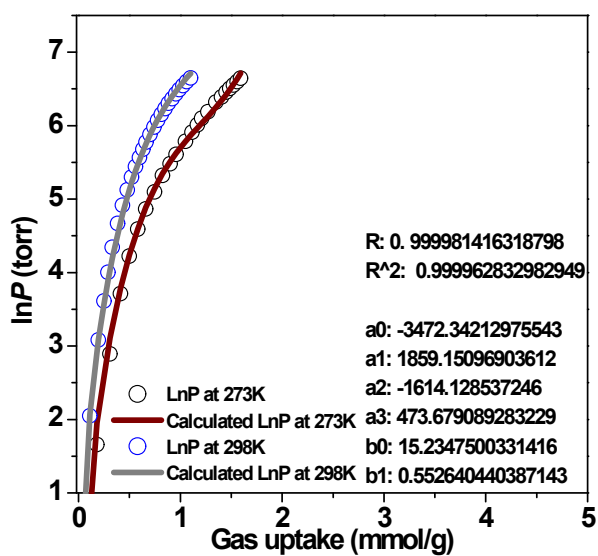


Figure S17 Curves fitting of C₂H₂ gas adsorption isotherms for NTU-56 at 273 K and 298 K.

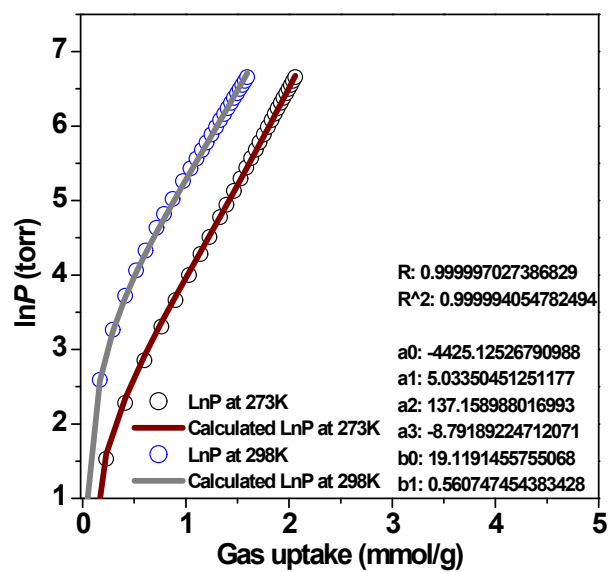


Figure S18 Curves fitting of CO_2 gas adsorption isotherms for NTU-57 at 273 K and 298 K.

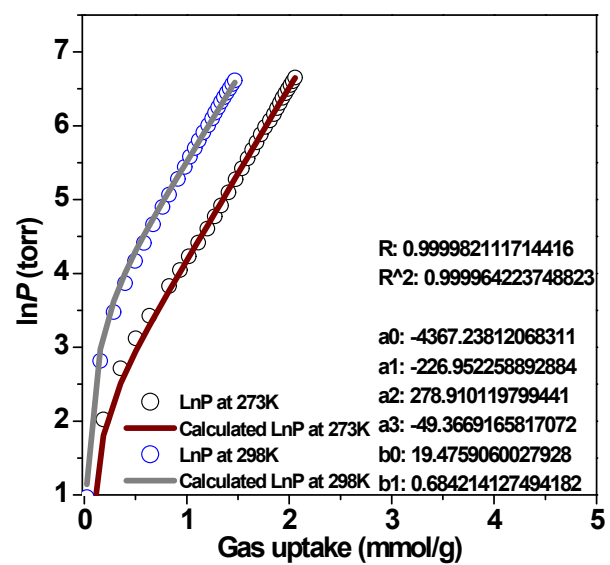


Figure S19 Curves fitting of C_2H_2 gas adsorption isotherms for NTU-57 at 273 K and 298 K.

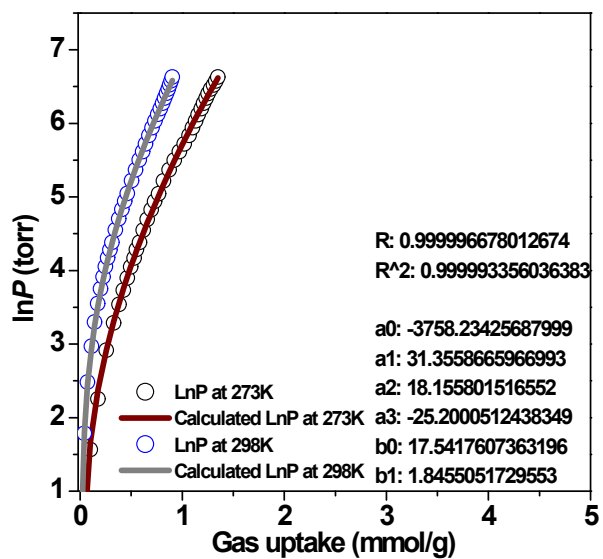


Figure S20 Curves fitting of CO₂ gas adsorption isotherms for NTU-58 at 273 K and 298 K.

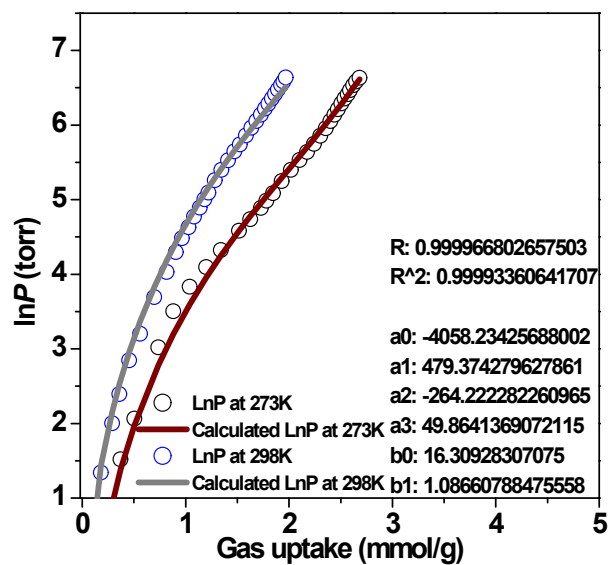


Figure S21 Curves fitting of C₂H₂ gas adsorption isotherms for NTU-58 at 273 K and 298 K.

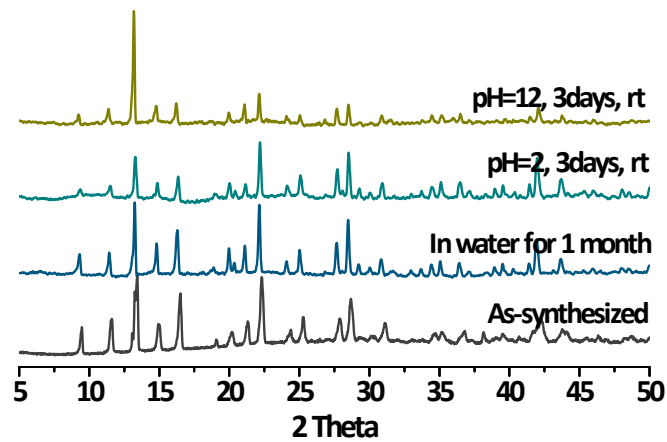


Figure S22 PXRD of water treated NTU-57.

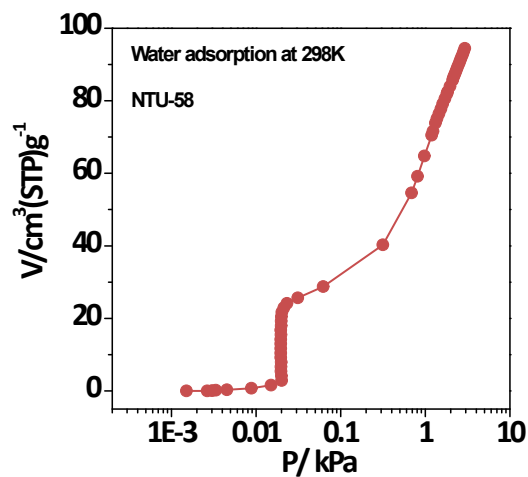


Figure S23 Water vapor adsorption of NTU-58. It shows two step uptakes, where the first quick uptake starts from about 200 Pa. However, the humidity of 18% was detected during the breakthrough experiment with water vapor, corresponding to 109.8 Pa for partial pressure of water. Although the temperature of the two experiments is different, we may infer that the relative low humidity may not open the framework during breakthrough experiment. Furthermore, the gap between crystals, as well as the surface of the stainless steel pipe wall, may be the space for water vapor, as the total amount of vapor is very small.